

AIRCRAFT OBSERVATIONS OF AIR MASS TRANSFORMATION OVER ADVANCING ICE COVER IN THE SEA OF OKHOTSK

*Jun Inoue¹, Masayuki Kawashima¹, Yasushi Fujiyoshi¹ and Masaaki Wakatsuchi^{1,2}

¹Institute of Low Temperature Science, Hokkaido Univ., Sapporo, Japan

²Core Research for Evolutional Science and Technology, Japan Science and Technology Corporation, Tokyo, Japan

1. INTRODUCTION

When a cold air mass breaks out from Siberia in winter, the air mass transformation occurs over the Sea of Okhotsk. As a result of heat and moisture supply from the ocean to the atmosphere, cloud streets form in the Sea of Okhotsk. However, the existence of sea ice in the Sea of Okhotsk suppresses heat exchange between air and sea surface. Therefore, it is expected that the cloud streets form not over the inner area of sea ice, but over the marginal ice zone of the Sea of Okhotsk. However, the cloud streets form over the inner area of sea ice where there are some fractures or leads in windward sea-ice area. This characteristic feature implies that considerable amounts of heat and moisture have been supplied to the atmosphere in the upstream ice covered area.

In case of the Sea of Okhotsk, the large heat release from leads or polynyas also occurs only during the cold-air outbreak. The cold incoming air experiences a strong temperature contrast at the surface when it encounters the leads or polynyas. As the air passes through the open water, it becomes warmer so that the air-sea temperature difference (i.e., sensible heat flux) decreases over the downwind leads and the lead-induced clouds form. These processes significantly change the heat balance in the marginal ice zone. The objective of this study is to reveal the role of open water area in the air mass transformation based on the aircraft observation which has been carried out over the southwestern part of Sea of Okhotsk in 14 February 2000.

2. AIRCRAFT OBSERVATION

We conducted aircraft observations during the cold-air outbreak on 14 Feb., 2000, using a Russian research aircraft ILYSHIN-18 (IL-18). The flight pattern of the aircraft IL-18 is shown in Figure 1. We had the aircraft observation with three measuring level flights (170, 350 and 850 m above the sea level) parallel to the wind direction at 850 hPa, that is, with the headings 290° and 110°. The horizontal length of each level flight was about 300 km. At starting and end points of the level flights, we did vertical soundings of the wind direction, wind speed, air temperature and dew point temperature.

The aircraft was equipped with gust probes to measure wind speed, wind direction, air temperature, humidity, dew point temperature, absolute humidity and pressure with 1-Hz and 20-Hz sampling frequencies. Furthermore, the aircraft IL-18 was equipped with instruments to measure all components of the radiation budget, liquid water content and cloud droplet concentration. A visible camera and an infrared camera were installed on the aircraft IL-18 to continuously record the characteristics of underlying surface conditions (e.g., size of sea ice, sea/ice surface temperature and amount of cloud).

3. SEA ICE CONDITION

We captured the sea-ice images every one second and made digital data with 720×480 pixels. The frame area corresponds to $120 \text{ m} \times 80 \text{ m}$ when the flight level was 170 m above the sea surface. Since sea ice has an insulating effect on the heat transfer, it is necessary to calculate the ice concentration precisely, using these sea ice images. The procedure to calculate the precise ice concentration is as follows, (1) quantify the brightness of images into 256 gray levels, (2) decide the threshold level between open water and sea ice, and (3) calculate the number of pixels that exceed the threshold level. Since the threshold level was not constant due to the sun glint, clouds and the shadow of sea ice and clouds, we determined the threshold level subjectively, and calculated the ice concentration for each image manually.

Figure 2a shows the change of ice concentration with the distance from the eastern coast of Sakhalin. Within 60 km from the coast, the ice concentration was almost 100 %. On the other hand, in the middle area, the mean ice concentration was reduced to approximately 70 %. Besides, there were some leads with less than 5 km in horizontal scale. The largest lead with little ripples was located at about 130 km offshore from the eastern coast of Sakhalin. The ice cover decreased rapidly in the downwind region. The fluctuation of the surface radiation temperature by using the infrared radiometer corresponds well to that of ice concentration (Figure 2b).

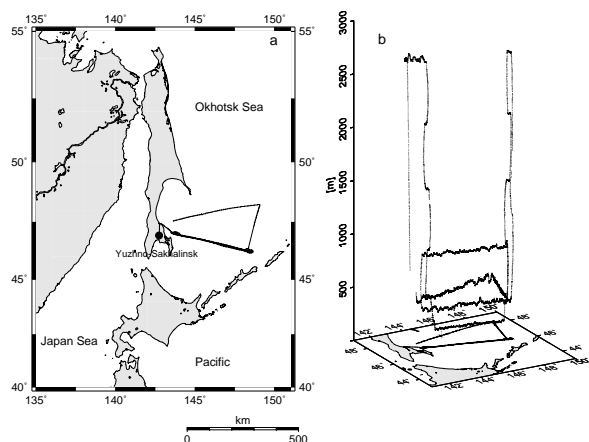


Figure 1: 2D (a) and 3D (b) schemes of the flight pattern of the research aircraft ILYSHIN-18 (IL-18) on 14 February 2000. Location of aerological station at Yuzhno-Sakhalinsk is shown by closed circle.

* Corresponding author address: Jun Inoue,

Institute of Low Temperature Science, Hokkaido Univ., Sapporo 060-0819, Japan; e-mail: inoue@lowtem.hokudai.ac.jp

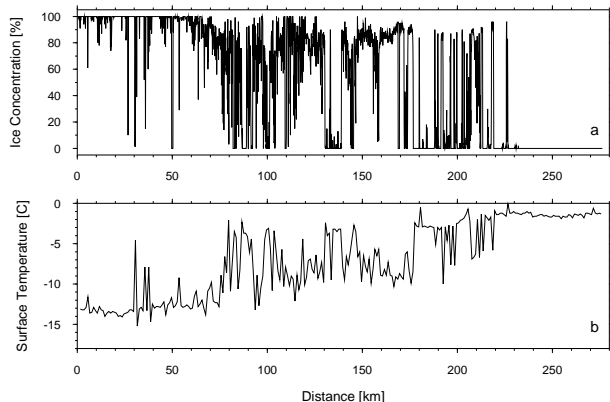


Figure 2: Horizontal distributions of (a) the ice concentration (%) derived from visible images of sea-ice and (b) sea/sea-ice surface temperature ($^{\circ}\text{C}$) derived from an infrared radiometer.

4. CONVECTION TRIGGERED BY LEADS

Glendening (1995) pointed out that there will be no strong convection over the lead if the across-lead wind U is strong or the width of lead is sufficiently small, because the air can pass through the lead without sufficient modification in such situations. He defined the critical lead width W for the atmospheric response by $W = U/N$, where N is the Brunt-Väisälä frequency. Under the cold-air outbreak situation in our case, the width W is approximately 4 km ($U = 8 \text{ m s}^{-1}$ and the stratification $\partial\theta/\partial z = 4 \text{ K km}^{-1}$). As shown in Figure 2a, the lead at about 130 km offshore from the eastern coast of Sakhalin (146.1°E) is wide enough ($> 4 \text{ km}$) to induce convection above it. Under cold-air outbreak situations in the Sea of Okhotsk, the advancing of ice cover should occur primarily through the ice advection by northwesterly wind (Kimura and Wakatsuchi, 1999), which makes lots of leads in the upstream region. Therefore, a detailed treatment of the ice concentration is necessary for detecting the location of strong convection and initiation of clouds over the ice covered area.

In order to investigate the heat flux as a function of fetch, i.e., accumulated open water width, we picked up ice-free area in Figure 2a and integrated the width of each open-water area by assuming that the horizontal scale of each image is 100 m. For a given sea surface temperature, -1.8°C (freezing point), we calculated the air-sea temperature difference. Figure 3 shows the temperature difference between the sea surface and atmosphere as a function of the accumulated fetch-width of open water. We can notice an initial steep and linear 2 K decrease in the temperature difference up to 35 km (from near the coast to 146.3°E ; Area I), beyond which the temperature difference becomes practically constant in a marginal ice zone between 35 km and 95 km (from 146.3°E to 147.6°E ; Area II). Over the open sea area from 95 km (from 147.6°E to 148.1°E ; Area III) the temperature difference gradually decreases again. These results show that the abrupt heating over the upstream leads induces a significant decrease of sensible heat flux downwind. Although the wide leads are important for the atmospheric convection, a linear relationship between the temperature difference and the accumulated width of leads in Area I suggests that the lead-effect on the sea-surface cooling depends not on the width of each lead, but on

the accumulated fetch-width of leads in ice covered area.

According to vertical soundings in the upstream and downstream region (Figure is not shown), the depth of boundary layer increased from 600 m to 1100 m. More than half of upstream region are covered with sea ice (Figure 2a), which causes a relatively small amount of turbulent heat flux to the atmosphere. Therefore, the main development of mixed boundary layer should occur in the downstream region. Once the mixed layer develops, it needs a relatively large amount of heat flux to keep its depth and to further develop. From the discontinuous point of the temperature difference between ocean and atmosphere at 146.3°E (Figure 3), the fluctuation of the air-sea temperature difference in Area II becomes larger than that in the upstream region (Area I) due to the strong turbulence. This result suggests again that the boundary layer rapidly developed within 20 km from a relatively large size of lead at 146.1°E .

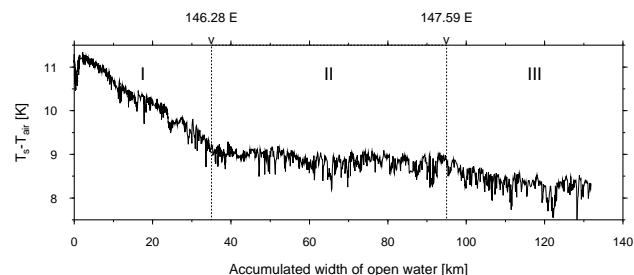


Figure 3: Temperature difference between sea surface temperature (-1.8°C) and air temperature (170 m level) as a function of accumulated width of open water. Broken lines denote the position in longitude. Areas I, II and III denote the open water area in ice covered area, marginal ice zone and open ocean, respectively.

5. CONCLUSIONS

Although the air mass was not modified sufficiently through the relatively narrow leads ($\leq 4 \text{ km}$) in the upstream region, the abrupt mixed layer development with lead-induced clouds occurred over the relatively wide lead. The air-sea temperature difference showed the linear decrease with the increase of the accumulated fetch-width of open water up to 35 km, beyond which the temperature difference became almost constant in the marginal ice zone due to the abrupt mixed layer development over the relatively wide lead. Considering that new-ice formation at the open water, i.e., polynyas and leads, depends on the temperature difference between the air and sea surface, the accumulated open water is one of important parameters to explain the advance of sea ice in the Sea of Okhotsk during the cold-air outbreaks thermodynamically.

REFERENCES

- Glendening, J. W., 1995: Horizontally integrated atmospheric heat flux from an Arctic lead. *J. Geophys. Res.*, **100**, 4613-4620.
- Kimura, N., and M. Wakatsuchi, 1999: Processes controlling the advance and retreat of sea ice in the Sea of Okhotsk. *J. Geophys. Res.*, **104**, 11137-11150.